



An Ultraviolet Excess in the Superluminous Supernova Gaia16apd Reveals a Powerful Central Engine

Citation

Nicholl, M., E. Berger, R. Margutti, P. K. Blanchard, D. Milisavljevic, P. Challis, B. D. Metzger, and R. Chornock. 2017. "An Ultraviolet Excess in the Superluminous Supernova Gaia16apd Reveals a Powerful Central Engine." *The Astrophysical Journal* 835 (1) (January 17): L8. doi:10.3847/2041-8213/aa56c5.

Published Version

doi:10.3847/2041-8213/aa56c5

Permanent link

<https://nrs.harvard.edu/URN-3:HUL.INSTREPOS:37373869>

Terms of Use

This article was downloaded from Harvard University's DASH repository, and is made available under the terms and conditions applicable to Open Access Policy Articles, as set forth at <http://nrs.harvard.edu/urn-3:HUL.InstRepos:dash.current.terms-of-use#OAP>

Share Your Story

The Harvard community has made this article openly available. Please share how this access benefits you. [Submit a story](#).

[Accessibility](#)

AN EXTREME ULTRAVIOLET EXCESS IN THE SUPERLUMINOUS SUPERNOVA GAIA16APD REVEALS A POWERFUL CENTRAL ENGINE

M. NICHOLL¹, E. BERGER¹, R. MARGUTTI², P. K. BLANCHARD¹, D. MILISAVLJEVIC¹, P. CHALLIS¹, B. D. METZGER³, R. CHORNOCK⁴

¹Harvard-Smithsonian Center for Astrophysics, 60 Garden Street, Cambridge, Massachusetts 02138, USA; matt.nicholl@cfa.harvard.edu

²Center for Interdisciplinary Exploration and Research in Astrophysics (CIERA) and Department of Physics and Astronomy, Northwestern University, Evanston, IL 60208

³Columbia Astrophysics Laboratory, Columbia University, New York, NY 10027, USA

⁴Astrophysical Institute, Department of Physics and Astronomy, 251B Clippinger Lab, Ohio University, Athens, OH 45701, USA

ABSTRACT

Since the discovery of superluminous supernovae (SLSNe) in the last decade, it has been known that these events exhibit bluer spectral energy distributions than other supernova subtypes, with significant output in the ultraviolet. However, the event Gaia16apd seems to outshine even the other SLSNe at rest-frame wavelengths below $\sim 3000 \text{ \AA}$. Yan et al. (2016) have recently presented *HST* UV spectra and attributed the UV flux to low metallicity and hence reduced line blanketing. Here we present UV and optical light curves over a longer baseline in time, revealing a rapid decline at UV wavelengths despite a typical optical evolution. Combining the published UV spectra with our own optical data, we demonstrate that Gaia16apd has a much hotter continuum than virtually any SLSN at maximum light, but it cools rapidly thereafter and is indistinguishable from the others by ~ 10 – 15 days after peak. Comparing the equivalent widths of UV absorption lines with those of other events, we show that the excess UV continuum is a result of a more powerful central power source, rather than a lack of UV absorption relative to other SLSNe or an additional component from interaction with the surrounding medium. These findings strongly support the central-engine hypothesis for hydrogen-poor SLSNe. An explosion ejecting $M_{\text{ej}} = 4(0.2/\kappa)M_{\odot}$, where κ is the opacity in $\text{cm}^2 \text{ g}^{-1}$, and forming a magnetar with spin period $P = 2 \text{ ms}$, and $B = 2 \times 10^{14} \text{ G}$ (lower than other SLSNe with comparable rise-times) can consistently explain the light curve evolution and high temperature at peak. The host metallicity, $Z = 0.18 Z_{\odot}$, is comparable to other SLSNe.

Keywords: supernovae: general — supernovae: Gaia16apd

1. INTRODUCTION

Superluminous supernovae (SLSNe) reach luminosities of $\sim 10^{44} \text{ erg s}^{-1}$, which is 10–100 times brighter than any previously known supernova (SN), and they are especially luminous in the UV (Quimby et al. 2011). While these explosions do seem to come from massive stars (Gal-Yam 2012; Nicholl et al. 2015), often following the loss of their hydrogen envelope (Inserra et al. 2013), the luminosity cannot be explained in the same way as for other core-collapse SNe: a shock depositing energy in the stellar envelope fails because the required efficiency is too large, and the mass of ^{56}Ni needed to power the light curve through radioactive decay often exceeds the total mass budget of the explosion. Instead, the debate has centred around whether the excess energy is input from an *external* source, such as the interaction of the SN ejecta with a massive shell of circumstellar material (CSM, e.g. Chevalier & Irwin 2011), or an *internal* engine, for which a highly magnetised neutron star remnant with a millisecond spin period seems to be the best candidate (Kasen & Bildsten 2010).

Gaia16apd was discovered by the Photometric Science

Alerts system from the *Gaia* survey (Wyrzykowski et al. 2012), and classified by the NOT Unbiased Transient Survey as a young, hydrogen-poor SLSN in a very faint galaxy at redshift $z = 0.102$ (Kangas et al. 2016). This makes it the second-nearest SLSN discovered to date. It quickly became clear that proximity was not the only thing that was special about this event—it was also extraordinarily UV-bright, being ~ 1.5 magnitudes brighter in the UV (~ 2000 – 3000 \AA) than the next-nearest SLSN, PTF12dam (Nicholl et al. 2013), despite a similar brightness in the optical. Recently, Yan et al. (2016) presented a detailed analysis of the UV spectrum of Gaia16apd at maximum light, showing that it was subject to significantly less line-blanketing than any normal-luminosity SNe, and hence likely metal-poor in the outer ejecta. While this may indeed explain why SLSNe in general are more UV-luminous than normal SNe, it does not tell the full story of Gaia16apd. In this paper, we show how its UV and optical evolution fit into the context of other SLSNe, with particular emphasis on what the UV diversity of these events can teach us of the power source. We argue that the observed properties can be accounted for self-

consistently by the popular magnetar model of SLSNe, and the UV excess in particular is a natural consequence of a short spin period and relatively low magnetic field in combination with a modest ejecta mass.

2. OBSERVATIONS

When Gaia16apd was announced, we immediately triggered follow-up observations from ground-based observatories and the *Swift* satellite. We obtained spectroscopic observations using the FAST and Blue Channel spectrographs on the 60" and MMT telescopes, respectively, at Fred Lawrence Whipple Observatory (FLWO); FAST spectra were reduced using a dedicated pipeline, while Blue Channel data were reduced in PYRAF. We show our spectra of Gaia16apd in Figure 1. We take the date of maximum light to be MJD 57541 for consistency with Yan et al. (2016).

The spectra are typical of hydrogen-poor SLSNe, as demonstrated by comparison to some of the best-observed events, showing the usual transition from a very blue spectrum with singly ionised oxygen to a redder spectrum dominated by iron and intermediate mass elements. Two of the best-observed low-redshift SLSNe are shown for comparison. Labels indicate the time in days with respect to r -band maximum light, in the SN rest-frame.

Imaging observations were obtained in optical passbands from the 48" imaging telescope at FLWO and de-biased/flat-fielded using ASTROPY packages. Photometry was determined by point-spread function fitting with a zero point derived from local field stars; the magnitudes of these stars were taken from the Pan-STARRS 3π survey where possible, or calibrated against standard fields on photometric nights in the case of B and V filters. Further photometry in the UV and optical were obtained with the UVOT instrument on *Swift* (Cycle 12 GI program #1215102) and extracted following Brown et al. (2009). Colour corrections¹ were applied to convert u, b, v magnitudes to the more standard U, B, V system. The earliest data points are from *Gaia* and PTF. We converted the *Gaia* G -band photometry to i -band using the observed $r-i$ colour and the post-launch colour-conversions from their Data Release 1². The PTF g -band point was presented by Yan et al. (2016). All data will be made available through the Open Supernova Catalog (Guillochon et al. 2016).

Our multicolour light curves are shown in Figure 2, highlighting the remarkable UV excess. We compare the colour evolution to other events with well-sampled UV light curves from *Swift*. PTF12dam (Nicholl et al. 2013) and SN 2015bn

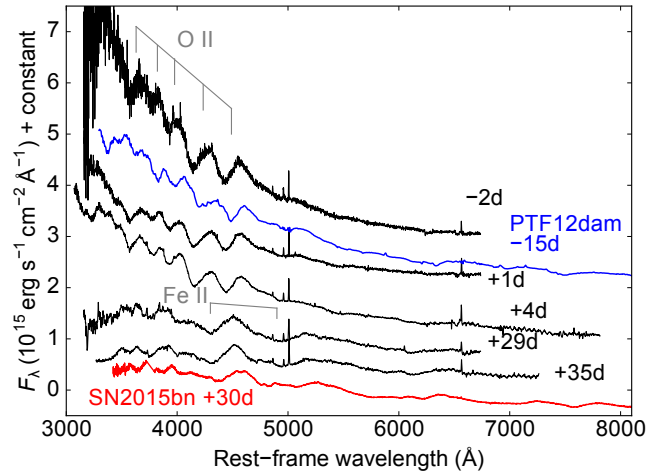


Figure 1. Spectroscopy of Gaia16apd. The optical spectra of Gaia16apd obtained from FAST and MMT show a typical evolution from a blue continuum with broad lines of singly-ionised oxygen to a redder spectrum dominated by iron and intermediate mass elements. Two of the best-observed low-redshift SLSNe are shown for comparison. Labels indicate the time in days with respect to r -band maximum light, in the SN rest-frame.

(Nicholl et al. 2016a) are both at similar redshift to Gaia16apd ($z \approx 0.1$), however we caution that SN 2010gx, at $z = 0.23$ (Pastorello et al. 2010), may be subject to a significant K -correction that is difficult to evaluate without UV spectra. The UV – $optical$ colours of Gaia16apd are bluer by 1–2 magnitudes at 20 days before r -band maximum, but evolve quickly such that by 10–15 days after maximum, all of the $z \approx 0.1$ events show near-identical colours. The convergence in colour suggests that the extinction in the host galaxy is indeed low, or at least similar to that in other SLSNe.

The optical $g-r$ colour evolution is perfectly consistent with the other events, demonstrating that if we had observed Gaia16apd only in the optical (or began UV follow-up shortly after maximum light), it would have looked like an entirely typical SLSN. The only other claimed SLSN with such an extreme UV – $optical$ colour is ASASSN-15lh (Dong et al. 2016). However, the interpretation of that event is contentious, and the spectroscopic evolution does not resemble the classic SLSN sequence shown in Figure 2 (Leloudas et al. 2016; Margutti et al. 2016). Thus Gaia16apd represents the first spectroscopically-normal SLSN to display this copious but rapidly-fading UV emission.

To demonstrate this more concretely, we plot a comparison of the spectral energy distribution (SED) for all SLSNe with available UV data in Figure 3, separating the data into early- and late-time observations. Gaia16apd was observed spectroscopically in the UV with the *Hubble Space Telescope* (*HST*) by Yan et al. (2016). The earliest UV spectrum was obtained on MJD 57541, approximately the time of bolometric maximum light, and thus during the UV-luminous phase, and further spectra were obtained at 11 and 25 days later. We downloaded these spectra from the *HST* archive and overplot them with the

¹ http://heasarc.gsfc.nasa.gov/docs/heasarc/caldb/swift/docs/uvot/uvot_caldb_coltrans_02b.pdf

² https://gaia.esac.esa.int/documentation/GDR1/Data_processing/chap_cu5phot/sec_phot_calibr.html#SS5

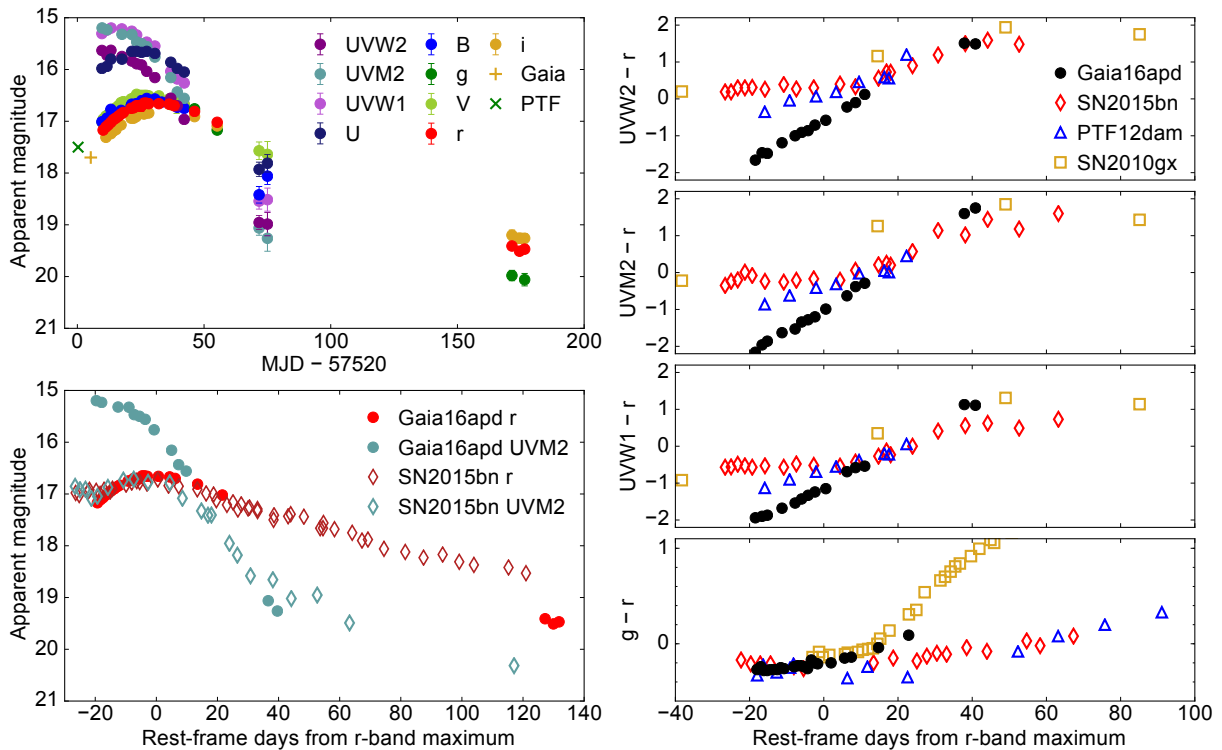


Figure 2. Optical and UV photometry of Gaia16apd. Top left: Multicolour lightcurves. Bandpasses are labelled in order from bluest to reddest. Note the initial brightness and rapid decline at UV wavelengths. Lower left: Comparison with SN2015bn (Nicholl et al. 2015), the best-observed SLSN to date, which is at a similar redshift ($z = 0.1136$) to Gaia16apd. Despite a similar r -band (optical) brightness, Gaia16apd is initially almost 2 magnitudes brighter in the UV. Right: Colour evolution of Gaia16apd compared to other low- z SLSNe. The $UV - optical$ colours redden from their extreme early values to look normal by 1–2 weeks after optical maximum light. Gaia16apd displays a typical $g - r$ colour evolution, as may be expected on the Rayleigh-Jeans tail of the SED.

SED derived from our *Swift* photometry. The flux calibration is consistent between the spectra and photometry.

It is clear that nearly all SLSNe display significant flux suppression below $\sim 3000 \text{ \AA}$ (though as pointed out by others, e.g. Quimby et al. 2011; Yan et al. 2016, less so than normal-luminosity SNe). This is true despite many of these objects being observed much earlier than Gaia16apd with respect to maximum light; early observations would favour bluer SEDs, as SNe almost universally cool with time. One notably blue SED is that of SNLS06d4eu (Howell et al. 2013). However, at $z = 1.588$, almost all of the data is rest-frame UV rather than optical, and the only spectrum obtained was at a very early phase of -17 days from peak. PS1-11bam, another high-redshift SLSN, seemed to show a blue continuum at maximum light (Berger et al. 2012; Yan et al. 2016), similar to Gaia16apd, but multicolour observations of this event are sparse.

For the late time comparison, we use the combined UV-optical SED at $+25$ – 29 d, scaled to the photometry at $+25$ d. The similarity to PTF12dam and SN2015bn at this phase agrees with our colour comparison, and shows that the UV properties of Gaia16apd are no longer out of the ordinary. The UV SED of SNLS06d4eu at maximum light matches other objects at later phases, showing that this event does not remain exceptionally UV-luminous for as long as Gaia16apd. PTF10hgi (Inserra et al. 2013) seems to be particularly UV-

faint for a SLSN.

3. THE NATURE OF THE UV EXCESS

We have so far demonstrated that Gaia16apd shows a pronounced UV excess at maximum light relative to other SLSNe, but that this emission fades to a more typical level shortly afterwards. Determining the source of the UV emission from Gaia16apd thus provides a new means to probe the physics of SLSNe.

Yan et al. (2016) propose that low metallicity is a key factor in explaining the copious UV flux in Gaia16apd. Using our three latest (deepest) spectra, we estimate the metallicity of the host galaxy from measured line ratios ($H\beta$, $[O II]$, $[O III]$). The common R_{23} diagnostic (assuming the lower branch; Kobulnicky et al. 1999), calibrated in the McGaugh (1991) scale, gives $12 + \log(O/H) = 7.94 \pm 0.06$, or $Z = 0.18 Z_{\odot}$. While this is at the low end for SLSN hosts, it is similar to various objects from Lunnan et al. (2014); Chen et al. (2015); Leloudas et al. (2015); Perley et al. (2016), and specifically the hosts of SN2010gx (Chen et al. 2013) and SN2015bn (Nicholl et al. 2016a). Yan et al. (2016) also note that the luminosity (a proxy for metallicity) of this galaxy in archival imaging is similar to other SLSN hosts. Moreover, the synthetic SLSN spectra from Mazzali et al. (2016) show only a modest change in the UV flux for models spanning an order of magnitude in metallicity.

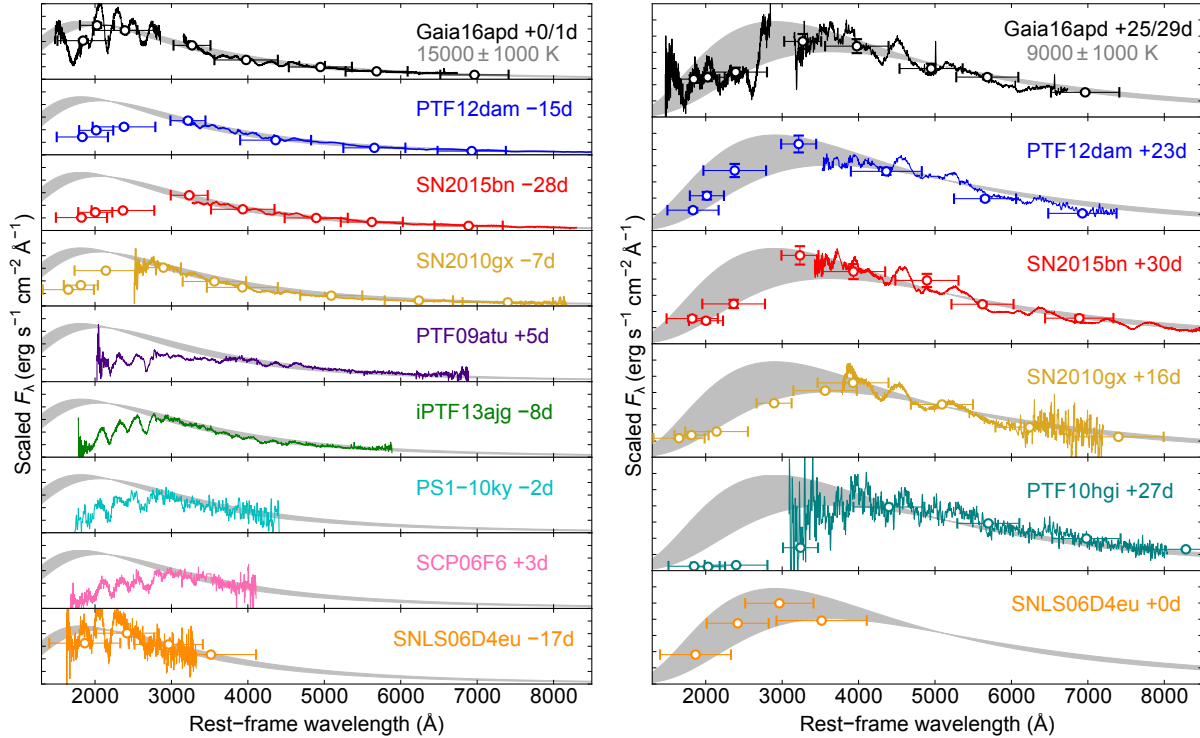


Figure 3. Left: The UV-optical SEDs of all SLSNe with broad wavelength coverage before or around maximum light. A 15000 K blackbody SED is shown for comparison. While this gives a good match to all SLSNe at wavelengths $\gtrsim 3000$ Å, most objects show a significant deficit in the UV compared to the blackbody. The photometry of Gaia16apd at maximum light, and SNLS06d4eu at very early times, are consistent with the blackbody curve, while their spectra suggest an even higher temperature. Right: The same comparison at several weeks after maximum (or at maximum for SNLS06d4eu). This time a blackbody of 8000–10000 K gives a reasonable approximation to the flux levels across the whole UV-optical regime for most SLSNe, including Gaia16apd. Data are from Nicholl et al. (2013, 2016a); Pastorello et al. (2010); Quimby et al. (2011); Vreeswijk et al. (2014); Chomiuk et al. (2011); Barbary et al. (2009); Howell et al. (2013); Inserra et al. (2013).

Thus metallicity alone cannot account for the UV excess.

One possibility is a short-lived additional energy source. In this interpretation, a high temperature would be required for the extra component such that most of the energy is emitted in the UV, which could point towards shock heating. While the timescale of the observed UV excess (a few weeks) is much too long for post-shock cooling of the stellar envelope—which expands rapidly and degrades the thermal energy content adiabatically—a shock passing through an extended CSM could generate a longer-lived high-temperature component. The other possibility is that there is only a single component to the luminosity, which peaks in the UV at early times and still manages to produce an optically-normal SLSN. We compare our multicolour photometry to blackbody models and do not find evidence for separate components with different temperatures (Figure 3). We therefore favour a single power source for the UV and optical emission. This requires that Gaia16apd has a hotter continuum temperature than other SLSNe at a similar phase from maximum light. Determining what sets this temperature will have important implications for understanding the underlying power source.

In a normal SN, the spectrum arises as an approximately thermal continuum, generated by electron scattering of photons in the optically-thick interior, and is then reprocessed by ab-

sorption and scattering from atomic lines in the lower-density outer ejecta. This fast-moving ejecta leads to absorption and P Cygni lines with Doppler widths characteristic of the ejecta velocity, $\sim 10^4$ km s $^{-1}$. The specific lines depend on the composition, ionisation and excitation of this line-forming region. Increasing the input power from a central source will generate a brighter continuum, but this will still be subject to the same absorption as it passes through the fast ejecta. On the other hand, if the luminosity is generated from interaction with an external CSM, the continuum is primarily generated above the region where broad lines form. Thus the spectrum will be a sum of the underlying SN spectrum and a bright thermal component. This has the unavoidable effect of diluting the lines relative to the continuum (e.g. Branch et al. 2000).

Whereas the pre-maximum optical spectra of SLSNe are largely featureless apart from the relatively shallow O II lines, the UV spectra show much stronger lines of ionised silicon, carbon, magnesium and titanium (Quimby et al. 2011; Vreeswijk et al. 2014; Mazzali et al. 2016). If Gaia16apd is powered by interaction with external material that generates a hotter continuum than in other SLSNe, peaking further into the UV, this should show up clearly as a decrease in the equivalent widths of these lines with respect to other events.

In Figure 4, we compare the *HST* spectra with the SLSN

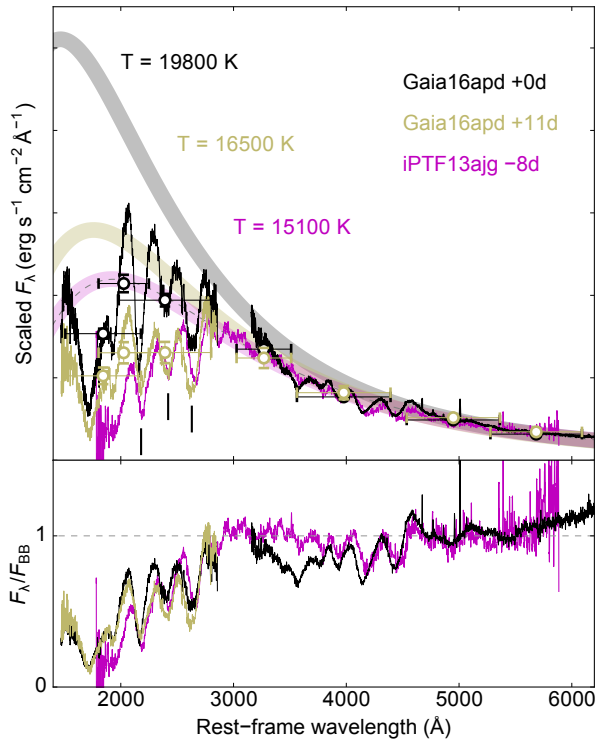


Figure 4. Normalising the UV-optical spectrum of Gaia16apd to a blackbody shows that a hotter underlying continuum is needed compared to other SLSNe. However, the equivalent widths of the lines are extremely similar to other SLSNe and show little evolution as the continuum fades. This suggests that the luminosity is processed through absorbing, fast-moving ejecta, thus favouring a central power source over external interaction.

iPTF13ajg (a spectroscopically typical event with good UV coverage, as shown in Figure 3). As discussed in section 2, the early UV photometry and maximum-light *HST* spectrum show that the SED turns over at $\sim 2000\text{\AA}$, compared to $\sim 3000\text{\AA}$ in iPTF13ajg. Despite this clear difference, the spectrum of Gaia16apd displays very deep, broad UV absorption lines that strikingly match those in iPTF13ajg. We measured the equivalent widths of the three strongest near-UV lines (marked on Figure 4) in both Gaia16apd and iPTF13ajg at the same phase relative to optical maximum. These lines have been identified by Mazzali et al. (2016) as blends of C II+C III+Ti III (2200\AA), C II+Ti III+Si II (2400\AA) and Mg II+C II (2670\AA). The equivalent width is defined as $W_\lambda = \int (F_\lambda - F_{\text{cont}}) / F_{\text{cont}} d\lambda$, where we approximate the continuum level, F_{cont} , as the tops of the absorption troughs (technically this is a ‘pseudo’-equivalent width). For these three features, we measure $W_\lambda \approx 59, 27, 51\text{\AA}$ for Gaia16apd, and $W_\lambda \approx 58, 28, 47\text{\AA}$ for iPTF13ajg. This similarity suggests that all of the additional energy in Gaia16apd is being reprocessed through the same absorbing SN ejecta as in iPTF13ajg, and thus the excess UV luminosity cannot be attributed to interaction with an external CSM.

We demonstrate this further with two additional observations, both shown in Figure 4. Firstly, we note that the spectrum of Gaia16apd at 11 d after maximum (when the UV ex-

cess has largely vanished from our photometry) is a very close match to that of iPTF13ajg—and the equivalent widths of the lines in Gaia16apd do not show a significant change despite a factor ~ 2 change in UV luminosity. Secondly, if we normalise the spectrum of Gaia16apd and iPTF13ajg by blackbody curves (using a temperature of $\sim 20000\text{ K}$ for Gaia16apd and $\sim 15000\text{ K}$ for iPTF13ajg), the resulting spectra look extremely similar. Thus the maximum-light UV spectrum of Gaia16apd can be explained by invoking the same absorption as other SLSNe but relative to a hotter continuum.

As pointed out by Yan et al. (2016), Gaia16apd emits around 50% of its maximum luminosity at wavelengths below 2500\AA . We have shown that this UV emission originates inside the fastest ejecta. Given that the UV luminosity alone would qualify Gaia16apd as super-luminous, this strongly favours the central engine scenario for the power source in Gaia16apd. The spectroscopic similarity to other SLSNe such as iPTF13ajg, after normalising to a hotter continuum, implies that the same mechanism is at work in the other hydrogen-poor SLSNe too. The question then is: which parameter(s) of the central engine model are able to generate a continuum in Gaia16apd that is much hotter at maximum light than almost any other event?

4. MAGNETAR MODEL AND IMPLICATIONS FOR SLSNE

We construct a model for Gaia16apd, assuming a millisecond magnetar as the power source. We first construct the bolometric light curve by converting our multi-band photometry to flux densities and shifting these to the SN rest frame. We integrate over the resultant SED and approximate missing flux outside of the observed bands using blackbody fits. We assume a constant bolometric correction for the earliest two points and upper limits (these limits are from Yan et al. 2016 and *Gaia*). This gives the light curve shown in Figure 5. We also plot SN 2015bn³ (Nicholl et al. 2016a) and SN 2010gx (Pastorello et al. 2010). The blackbody fits allow us to derive the evolution of the colour temperature and radius (note that this temperature is different to the suggested unabsorbed blackbodies in Figure 4), which will serve as important points of comparison for modelling.

We fit the light curve using the magnetar model first presented by Inserra et al. (2013). Fixing the velocity to 10000 km s^{-1} at the edge of the dense core, the photospheric velocity at maximum light is $\sim 14000\text{ km s}^{-1}$ for their assumed density profile, in good agreement with that measured by Yan et al. (2016). We find an excellent fit to the bolometric light curve over a period of 150 d. The best-fitting free parameters are as follows: ejected mass $M_{\text{ej}} = 4.0 M_\odot$ for an opacity $\kappa = 0.2\text{ cm}^2\text{ g}^{-1}$; magnetic field $B = 2.0 \times 10^{14}\text{ G}$; and spin period $P = 2.1\text{ ms}$. If the opacity is instead $0.1\text{ cm}^2\text{ g}^{-1}$, the inferred ejecta mass increases to $8 M_\odot$ —closer to the $12 M_\odot$ estimated by Yan et al. (2016) for this opacity.

³ We correct an error in Nicholl et al. (2016a), where the radius in Figure 17 was too high by a factor $\sqrt{\pi}$

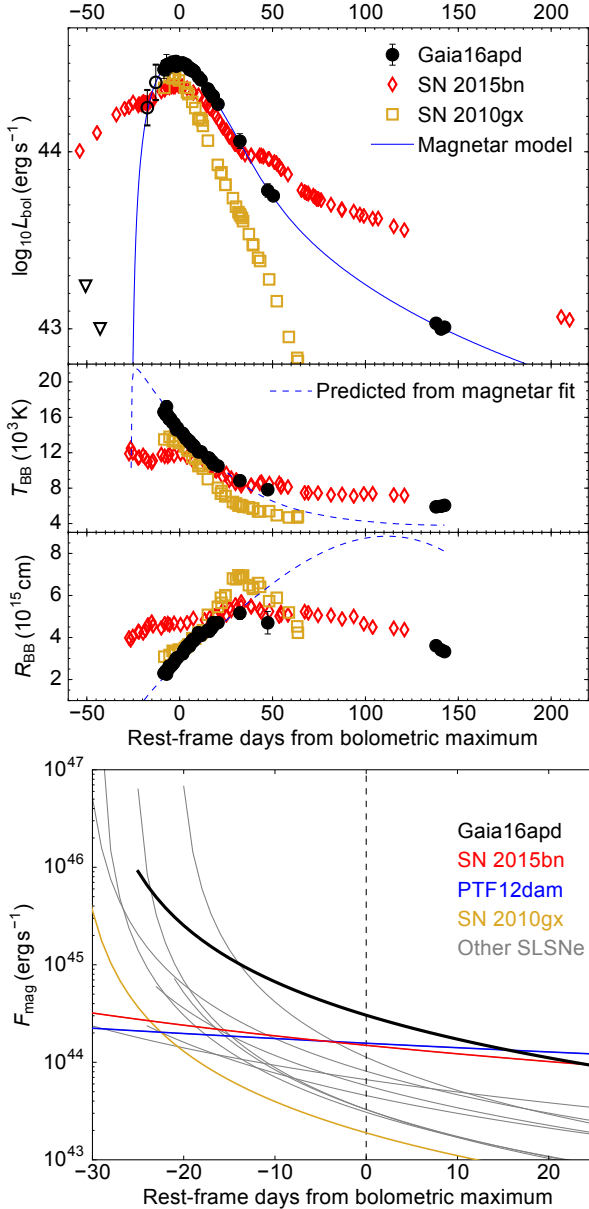


Figure 5. Top: The bolometric light curve and blackbody temperature/radius evolution of Gaia16apd, compared with SLSNe 2015bn and 2010gx, and magnetar model fit. Bottom: The derived magnetar parameters for Gaia16apd predict a more powerful engine than any other SLSN over the period where the UV excess is observed.

The kinetic energy in our model, $2.4 \times 10^{51} \text{ erg}^4$, is much smaller than that estimated by those authors, who found $E > 10^{52} \text{ erg}$. The main reason for this is that most of the ejecta behind the photosphere in our model, assuming homologous expansion, are at velocities $\ll 14000 \text{ km s}^{-1}$. Given that a central engine is thought to inflate a bubble inside the ejecta (Kasen & Bildsten 2010; Woosley 2010), homology may be a coarse assumption. The true kinetic energy likely resides somewhere between our estimate and that of Yan et al. (2016),

⁴ We find essentially the same energy if we fix the explosion to 10^{51} erg and add a contribution from the magnetar following Inserra et al. (2013).

but seems to be at least a few times 10^{51} erg —higher than in a canonical SN.

The model gives a good match to the radius and effective temperature of Gaia16apd until about a month after maximum light. The fit becomes poor at much later times, when the measured temperature and radius are relatively constant compared to the model. This may be attributable to the simplicity of our assumed density distribution, or multidimensional effects.

The physical reason for the high temperature is revealed by our fit parameters: Gaia16apd falls in a seemingly unusual ‘sweet spot’, as we will now demonstrate. Following Kasen & Bildsten (2010), the magnetar spin-down timescale is

$$\tau_{\text{sd}} = 4.7(B/10^{14} \text{ G})^{-2}(P/\text{ms})^2 \text{ d}, \quad (1)$$

and the power function, which is the heating term in the light curve integral (Arnett 1982), is given by

$$F_{\text{mag}}(t) = 4.9 \times 10^{46} \left(\frac{B}{10^{14} \text{ G}} \right)^2 \left(\frac{P}{1 \text{ ms}} \right)^{-4} \left(1 + \frac{t}{\tau_{\text{sd}}} \right)^{-2}. \quad (2)$$

For a given τ_{sd} , the early-time power input is maximised by minimising the spin period⁵. However, more powerful magnetars also spin down more quickly according to equation 1.

We compile a comparison sample of all low-redshift SLSNe that have been fit with the same magnetar model in the literature: SN 2015bn, PTF12dam, SN 2010gx, PS1-11ap (McCrum et al. 2014), the 5 objects from Inserra et al. (2013), and the 3 objects from Nicholl et al. (2014). We observe that in all SLSNe with magnetar model fits, those with the long rise times (typically more massive ejecta) tend to have $B \approx 10^{14} \text{ G}$, which is a factor of $\sim 4\text{--}8$ weaker than in the fast-rising (lower-mass) events. Gaia16apd is unusual in that it has a rise time of 26 d (at the short end for SLSNe; Nicholl et al. 2015) in combination a fairly low magnetic field, $B = 2 \times 10^{14} \text{ G}$. This gives a longer τ_{sd} (5.6 d) than other SLSNe of comparable rise time. The short spin period of 2 ms (the physical lower limit is $\approx 1 \text{ ms}$; e.g. Metzger et al. 2015) is faster than in some events, though many others have a comparable period.

Using the observed rise times and the fitted B and P , we use equation 1 to determine $F_{\text{mag}}(t)$ for each SLSN (bottom of Figure 5). For around 2 weeks at either side of maximum light, Gaia16apd has a power source that is $\gtrsim 2$ times more energetic than any other event. The UV spectral models for SLSNe presented by Howell et al. (2013, their Figure 11) show how, for all other things equal, a more powerful central source gives a bluer UV spectrum exactly as we observe. Nicholl et al. (2016a) pointed out that slowly-fading SLSNe like SN 2015bn stay blue for much longer than other SLSNe; this is consistent with the fact that beyond $\sim 20 \text{ d}$ after maximum light SN 2015bn and PTF12dam have the largest F_{mag} .

The early UV excess in Gaia16apd also owes to the short rise time. Figure 5 shows that the ejecta are still relatively compact

⁵ At later times, $t \gg \tau_{\text{sd}}$, the dependence on P cancels out, and equations 1 and 2 together yield $F_{\text{mag}} \propto B^{-2}$. Diversity in B thus gives the fast and slowly-declining types of SLSNe (Nicholl et al. 2013).

at maximum light (e.g. compared to SN 2015bn); if we assume an underlying blackbody SED then a higher temperature naturally follows from injecting this much energy into a modest radius. After a few weeks from maximum light, both the measured radius and inferred engine power are similar between Gaia16apd and SN 2015bn, consistent with the convergence in their colour evolution (Figure 2).

It is important to remember that this analysis has stemmed simply from a magnetar model fit to the bolometric light curve of Gaia16apd, with no constraints on the colours. That the derived parameters give a complete and straight-forward explanation for the UV excess (and in fact the relative colour evolution of both fast and slow SLSNe) therefore constitutes strong evidence in favour of the magnetar model. It is also possible that another type of engine could generate the same behaviour (e.g. Dexter & Kasen 2013; Gilkis et al. 2016), but we suggest that any such model would require two free parameters to set the engine’s luminosity and timescale (in addition to the ejecta mass) in order to simultaneously reproduce the diversity in bolometric and colour evolution in the SLSN population.

5. CONCLUSIONS

Despite an apparently normal evolution in the optical, Gaia16apd is the most UV-luminous SLSN yet discovered (excepting the controversial ASASSN-15lh). While low metallicity likely is a factor in the overall UV-brightness of SLSNe relative to normal SNe, as suggested by Yan et al. (2016) and Mazzali et al. (2016), this alone does not account for the diverse UV luminosities within the SLSN class, since Gaia16apd shows the same degree of absorption as other objects that are much less luminous in the UV. In fact, the equivalent widths of the UV absorption lines and their evolution compared to other SLSNe seem to necessitate a powerful central energy source.

Building a model for the light curve, we showed that one can self-consistently explain both the overall luminosity and the UV excess of Gaia16apd in a magnetar-powered explosion. The key properties are a *short spin period* setting a high overall energy scale, relatively *low mass* giving a short rise time and thus a smaller radius (corresponding to a higher temperature) at maximum light, and most importantly a *weaker magnetic field* than any other fast-rising event, increasing the spin-down time so that more power is injected around peak.

Taking this result along with other recent observational progress, such as the link between the nebular spectra of SLSNe and gamma-ray burst SNe (Nicholl et al. 2016b; Jerkstrand et al. 2016), and theoretical work in magnetar formation (Mösta et al. 2015), it now seems clear that a central engine—most likely a millisecond magnetar—is the power source in hydrogen-poor SLSNe.

Another important implication of these results is the need to follow up all SLSNe at UV wavelengths. UV data for nearby SLSNe is still fairly sparse, yet clearly the optical data for Gaia16apd told only part of the story. The discovery that some SLSNe are this bright in the UV is a major boost for future

high-redshift searches. JWST should easily detect Gaia16apd-like events at $z \gtrsim 10$ as approximately year-long near-infrared transients (unlike pair-instability SNe, which would have much longer timescales and should be faint in the rest-frame UV), offering perhaps the most promising opportunity yet to observe the deaths of the first stars.

R.M. acknowledges generous support from NASA Grant NNX16AT81G.

REFERENCES

- Arnett, W. D. 1982, ApJ, 253, 785
 Barbary, K., Dawson, K. S., Tokita, K., et al. 2009, ApJ, 690, 1358
 Berger, E., Chornock, R., Lunnan, R., et al. 2012, ApJL, 755, L29
 Branch, D., Jeffery, D. J., Blaylock, M., & Hatano, K. 2000, PASP, 112, 217
 Brown, P. J., Holland, S. T., Immler, S., et al. 2009, The AJ, 137, 4517
 Chen, T.-W., Smartt, S. J., Bresolin, F., et al. 2013, ApJ, 763, L28
 Chen, T.-W., Smartt, S. J., Jerkstrand, A., et al. 2015, MNRAS, 452, 1567
 Chevalier, R. A., & Irwin, C. M. 2011, ApJL, 729, L6
 Chomiuk, L., Chornock, R., Soderberg, A., et al. 2011, ApJ, 743, 114
 Dexter, J., & Kasen, D. 2013, ApJ, 772, 30
 Dong, S., Shappee, B. J., Prieto, J. L., et al. 2016, Science, 351, 257
 Gal-Yam, A. 2012, Science, 337, 927
 Kasen, D., Soker, N., & Papish, O. 2016, ApJ, 826, 178
 Guillochon, J., Parrent, J., & Margutti, R. 2016, arXiv:1605.01054
 Howell, D., Kasen, D., Lidman, C., et al. 2013, ApJ, 779, 98
 Inserra, C., Smartt, S., Jerkstrand, A., et al. 2013, ApJ, 770, 128
 Jerkstrand, A., Smartt, S., Inserra, C., et al. 2016, arXiv:1608.02994
 Kangas, T., Elias-Rosa, N., Lundqvist, P., et al. 2016, The Astronomer’s Telegram, 9071
 Kasen, D., & Bildsten, L. 2010, ApJ, 717, 245
 Kobulnicky, H. A., Kennicutt Jr, R. C., & Pizagno, J. L. 1999, ApJ, 514, 544
 Leloudas, G., Schulze, S., Krühler, T., et al. 2015, MNRAS, 449, 917
 Leloudas, G., Fraser, M., Stone, N., et al. 2016, arXiv:1609.02927
 Lunnan, R., Chornock, R., Berger, E., et al. 2014, ApJ, 787, 138
 Margutti, R., et al. 2016, arXiv:1610.01632
 Mazzali, P., Sullivan, M., Pian, E., Greiner, J., & Kann, D. 2016, Monthly Notices of the Royal Astronomical Society, 458, 3455
 McCrum, M., Smartt, S., Kotak, R., et al. 2014, MNRAS, 437, 656
 McGaugh, S. S. 1991, ApJ, 380, 140
 Metzger, B. D., Margalit, B., Kasen, D., & Quataert, E. 2015, MNRAS, 454, 3311
 Mösta, P., Ott, C. D., Radice, D., et al. 2015, Nature, 528, 376
 Nicholl, M., Smartt, S. J., Jerkstrand, A., et al. 2013, Nature, 502, 346
 —. 2014, MNRAS, 444, 2096
 —. 2015, MNRAS, 452, 3869
 Nicholl, M., Berger, E., Smartt, S. J., et al. 2016a, ApJ, 826, 39
 Nicholl, M., Berger, E., Margutti, R., et al. 2016b, ApJL, 828, L18
 Osterbrock, D. E. 1989, Astrophysics of gaseous nebulae and active galactic nuclei
 Pastorello, A., Smartt, S., Botticella, M., et al. 2010, ApJL, 724, L16
 Perley, D. A., Quimby, R., Yan, L., et al. 2016, arXiv:1604.08207
 Poznanski, D., Prochaska, J. X., & Bloom, J. S. 2012, MNRAS, 426, 1465
 Quimby, R. M., Kulkarni, S., Kasliwal, M. M., et al. 2011, Nature, 474, 487
 Schlafly, E. F., & Finkbeiner, D. P. 2011, ApJ, 737, 103
 Vreeswijk, P. M., Savaglio, S., Gal-Yam, A., et al. 2014, ApJ, 797, 24
 Woosley, S. 2010, ApJL, 719, L204
 Wyrzykowski, L., Hodgkin, S., Blogorodnova, N., Kozlov, S., & Burgon, R. 2012, arXiv:1210.5007
 Yan, L., Quimby, R., Gal-Yam, A., et al. 2016, arXiv:1611.02782